

Upsampling of Prostate Volumes

Joseph Marino and Arie Kaufman, *Fellow, IEEE*

Department of Computer Science and CEWIT

Stony Brook University

Stony Brook, NY 11794-4400, USA

{jmarino, ari}@cs.stonybrook.edu

Abstract—The application of magnetic resonance imaging (MRI) in detecting and localizing prostate cancer lends itself naturally to 3D volume rendering, allowing the physician to observe the entire gland and navigate at will. While MR images can be obtained with good intra-slice resolution, inter-slice gaps are significantly larger. Because of this, when visualizing a prostate segmented from MR image slices in 3D, the result is very faceted. In addition to the overall gland, a further item of concern is the separate segmentation of the peripheral zone (PZ) from the central gland (CG). As these two regions present different characteristics in the MR images, it is important to keep them separated in the segmentation, so any upsampling of the gland must also upsample the CG and PZ region segmentations while preserving the entire gland segmentation. A first step is to increase the inter-slice resolution of the volume by interpolating intermediate slices. This is accomplished by iterative erosion and dilation of regions to ensure that both the overall and region segmentations are maintained. This is performed multiple times, until the inter-slice spacing is reduced to the level of the intra-slice spacing. Rendering a volume upsampled this way will produce better results, but there will still be a blocky step-like appearance, though now reduced to smaller steps. In prostate imaging, it is common to acquire slices in axial, coronal, and sagittal views. Combining these three views together allows for a superior result which is significantly smoother. Another advantage is that the final shape can be more accurate, as small areas around the boundary that may not be segmented properly due to their appearance in one view can be contributed to the final volume by an alternate view.

Keywords—prostate; medical imaging; interpolation; volume rendering; visualization;

I. INTRODUCTION

Prostate cancer (CaP) is the most incident cancer and the second leading cause of cancer related mortality for males in the United States [4]. It has been noted that magnetic resonance imaging (MRI) can be used for the detection of CaP [3], though multiple MR images obtained with different settings are necessary. Most commonly used is a combination of T_2 -weighted and T_1 -weighted image sequences. T_2 -weighted images, which provide better imaging quality of the prostate gland, are generally used to locate regions suspected of being cancerous, while T_1 -weighted images are used to discount false positives, primarily due to the presence of post-biopsy hemorrhaging. Other methods of MR imaging, including MR spectroscopic imaging (MRSI), diffusion-weighted imaging (DWI), and dynamic contrast enhancement (DCE) have also been suggested for CaP detection. However, these modes in general do

not add to the structural shape of the gland and are thus not addressed in this work.

The use of MR image sequences for CaP detection leads naturally to the use of 3D volume rendering visualization methods for viewing the data. However, the acquired MR sequences often have very low z-resolution (that is, a high inter-slice spacing), and thus a 3D volume rendering of the segmented prostate gland from these scans as-is will appear with large stepping artifacts. Due to this, we present here a simple and fast method to first upsample the prostate segmentation labelmap slices and then combine three orthogonal views into a single composite labelmap such that a smoother and more realistic rendering can be achieved.

II. RELATED WORK

Due to the low z-resolution of MR image sequences, a shape based interpolation method is necessary to recreate intermediate slices and make the resolution near isotropic. One method of upsampling is to perform grey-level interpolation to create new images slices [1]. However, this increases the amount of segmentation work that would need to be performed. Rather, we are interested in a method for interpolating slices of segmented volumes. Common methods for this take as input a binary segmentation [5] or a threshold that allows for a binary segmentation of the data [2]. However, for our work it is necessary to maintain a ternary segmentation, and thus we present a ternary shape based segmentation interpolation method in which known regions are dilated into unknown regions to form the final shape in an interpolated slice. We further take into account information from multiple labelmaps to create the final upsampled labelmap. Our method is fast, easy to implement, and suitable for CaP visualization needs.

III. MEDICAL BACKGROUND

For work related to the detection of CaP from MR images, an understanding of prostate zonal anatomy is necessary. The prostate is divided into three zones, referred to as the peripheral zone (PZ), transitional zone (TZ), and central zone (CZ), with the PZ being the largest, accounting for approximately 70% of the prostate and also 70% of cancer cases [6]. In contrast to the PZ, the TZ and CZ are often considered together as a single region, and as such are referred to as the central gland (CG).

T_2 -weighted images provide good image quality of the prostate gland, allowing for a differentiation between the PZ and CG. For normal prostatic tissue, the PZ will demonstrate

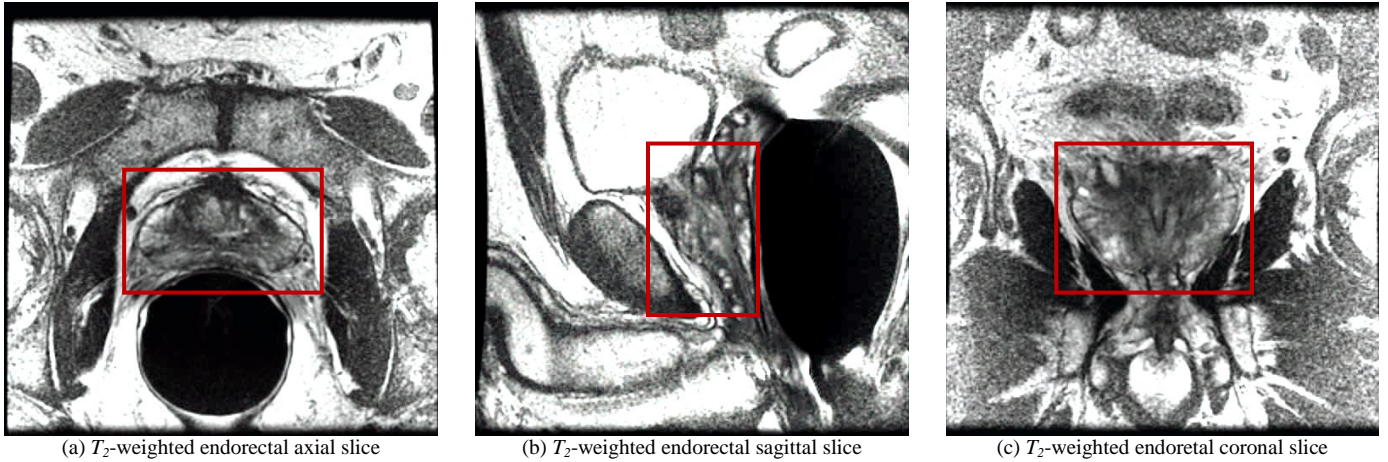


Figure 1. Sample slices from each of the three MR image sequences used in this work. The area containing the prostate is outlined by a red box.

high signal intensity in the T_2 -weighted images. In cancerous tissue, the PZ will generally demonstrate decreased signal intensity. In the CG, however, normal tissue already demonstrates low signal intensity. Due to this, detection of CaP in the CG based on intensity is not feasible, and thus individual segmentations of PZ and CG must be determined and maintained. T_1 -weighted images are also acquired and used to discount false positives due to hemorrhaging from previous needle biopsies. However, the CG and PZ are not differentiable in T_1 -weighted images and the slices are from external pelvic acquisitions, and thus larger. Due to this, the T_1 -weighted images are not suitable for extracting the shape of the prostate and are not used in this work.

We use three T_2 -weighted image sequences which are approximately orthogonal, so that the final shape from the segmentations and upsampling is as accurate as possible. Specifically, the three scans used are a T_2 -weighted endorectal axial scan, a T_2 -weighted endorectal coronal scan, and a T_2 -weighted endorectal sagittal scan. A sample slice from each of these scans is shown in Fig. 1. The relationship between the scans is shown in Fig. 2, with the axial slice outlined in blue, the sagittal slice in red, and the coronal slice in purple. Also shown is a T_1 -weighted slice, outlined in green. For these T_2 -weighted image sequences, the data was generally acquired with approximately 0.55 mm intra-slice and 3 mm inter-slice spacing. These scans were acquired during a single session without patient movement, and thus are naturally aligned using their position and orientation information.

IV. PREPROCESSING

As input into our work we take hard segmented volumes of all three orientations of T_2 -weighted data (axial, coronal and sagittal). These segmentations are in the form of ternary labelmaps. These labelmap volumes contain ternary segmentation information, rather than simply a binary segmentation, because we take into account the zonal anatomy of the prostate. Each labeled voxel is indicated as either not belonging to the prostate, belonging to the region of the PZ, or belonging to the remaining portion on the gland. This remaining portion technically contains both the CG region and the fibromuscular stroma, though from hereafter we will refer to this labeled re-

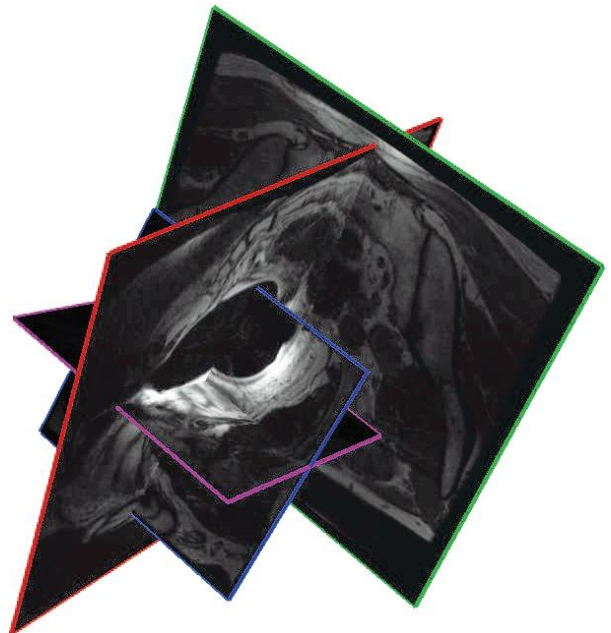


Figure 2. Example of the relative position and orientation of the four image sequences acquired for a prostate dataset and how they are naturally registered in the world space. The single T_1 -weighted sequence (outlined in green) is much larger and of coarser resolution than the T_2 -weighted scans.

gion simply as the CG region for the sake of brevity. For our current work, these segmentations are obtained manually as the segmentation itself is outside the scope of our work.

Using the image position, resolution, and orientation information from the DICOM data, the image volumes can be aligned properly in 3D space with respect to each other. An example of this accurate alignment of the four image sequences of one dataset is shown in Fig. 2. Because of this alignment, we do not need to perform registration, and corresponding voxel positions can be easily found between the three volumes.

V. LABELMAP UPSAMPLING

The first part of our upsampling method is to upsample each T_2 -weighted ternary labelmap volume separately along its z -axis by interpolating new slices in order to reduce the inter-



Figure 3. Example of the ternary labelmap interpolation. The PZ label is indicated by red and the CG by green. (a) and (b) Two neighboring slices from the original labelmap volume. (c) Interpolated slice when the PZ and CG regions are interpolated separately, resulting in a large missing area where the prostate should be. (d) Result from our ternary method, where the shape of the overall prostate segmentation has been preserved and no prostate area is missing.

slice spacing to the level of the intra-slice spacing. We encode the ternary segmentation into the voxels as follows: voxels not belonging to the prostate are assigned a value of 0, voxels belonging to the PZ are assigned a value of 10, and voxels belonging to the CG are assigned a value of 30. The result of our upsampling will likewise contain only these three values when completed. We have developed a simple method based on iterative erosions and dilations which will take this ternary data into account, preserving the shape of the entire gland as well as of the individual zonal regions.

An interpolated slice is created midway between each pair of neighboring slices in the original labelmap volume. The algorithm contains four steps which are performed on the interpolated slice that is to be created. These four steps can be repeated as needed to reduce the inter-slice spacing of the volume to the level of the intra-slice spacing. For the discussion that follows, the use of the term neighboring voxels refers to the two neighboring voxels from the two neighboring slices. That is, given two slices A and B, for the interpolated slice AB between A and B, a voxel v_{AB} with position (x, y) in the interpolated slice contains two neighbor voxels v_A and v_B with position (x, y) in slices A and B, respectively.

The first step in this algorithm is an initial labeling of all voxels in the interpolated slice. For every voxel v_{AB} in the interpolated slice, its value is set to be the mean of the two neighboring voxels, v_A and v_B . If both neighboring voxels are labeled as non-prostate, then the corresponding interpolated voxel must also be non-prostate and is correctly labeled 0. If both neighboring voxels are either PZ or CG, then the corresponding interpolated voxel must also be PZ or CG, and it is correctly labeled as 10 or 30, respectively. If one neighboring voxel is PZ and the other is CG, then the interpolated voxel will certainly be in the prostate, but it is as yet undetermined as to whether it should be labeled as PZ or CG (its current value is set to 20). If the interpolated voxel is between a prostate voxel and a non-prostate voxel, then it will be labeled as uncertain (value of 5 or 15) and will be further processed.

The second step is an erosion of the areas that have been labeled as uncertain (labeled as 5 or 15); that is, areas that could be inside or outside of the prostate. If an area is known to belong to the prostate, it is referred to as certain (note that voxels which must belong to the prostate but can be either PZ or CG are referred to as certain but undetermined). The uncertain regions are eroded by performing iterative dilations on the

certain regions into the uncertain regions. After this step, all voxels in the interpolated slice will be labeled as one of the four certain types. Note that the undetermined voxels (labeled as 20) are also dilated, such that they grow outwards from their initial locations, as this is important for the next step.

The third step is to re-label voxels as belonging to the PZ or CG. For this, a decision is made for all of the undetermined voxels (labeled as 20). Since this region was grown during the previous step, some of these undetermined voxels will now have a prostate label in one neighboring slice and a non-prostate label in the other neighboring slice. Since these voxels are certain to be contained within the prostate, we label them with the PZ or CG label from its corresponding prostate neighbor (value 10 or 30).

The final step for the z -resolution upsampling is a further erosion of the remaining undetermined voxels (labeled as 20), which are guaranteed to belong to the prostate but are not yet labeled as PZ or CG. These voxels are eroded similarly to the second step above, though only the PZ labels (value of 10) and CG labels (value of 30) are allowed to grow into them, as it is known that the voxel must belong to the prostate and thus the non-prostate voxels (value of 0) are not allowed to grow into them. After this step, all voxels in the prostate will be labeled as belonging to either the PZ or CG.

After these four steps, every voxel will be labeled as either non-prostate (value of 0), PZ region (value of 10), or CG region (value of 30), preserving the ternary state of the labelmap. This method is necessary instead of a conventional binary shape-based interpolation approach in order to avoid gaps. If each prostate region (PZ and CG) is interpolated separately, gaps can occur in the resulting interpolated labelmap that should be covered by the prostate. An example of this problem is shown in Fig. 3. This interpolation is repeated until the z -resolution of each labelmap volume is no worse than twice its corresponding x - and y -resolutions.

VI. COMPOSITE LABELMAP

The second part of the upsampling algorithm is to create a composite upsampled labelmap volume. All three upsampled labelmap volumes from the T_2 -weighed data are used in creating this composite volume, capitalizing on the good intra-slice resolution of the generally orthogonal datasets. That is, if we take the axial volume as the canonical orientation for xyz , then

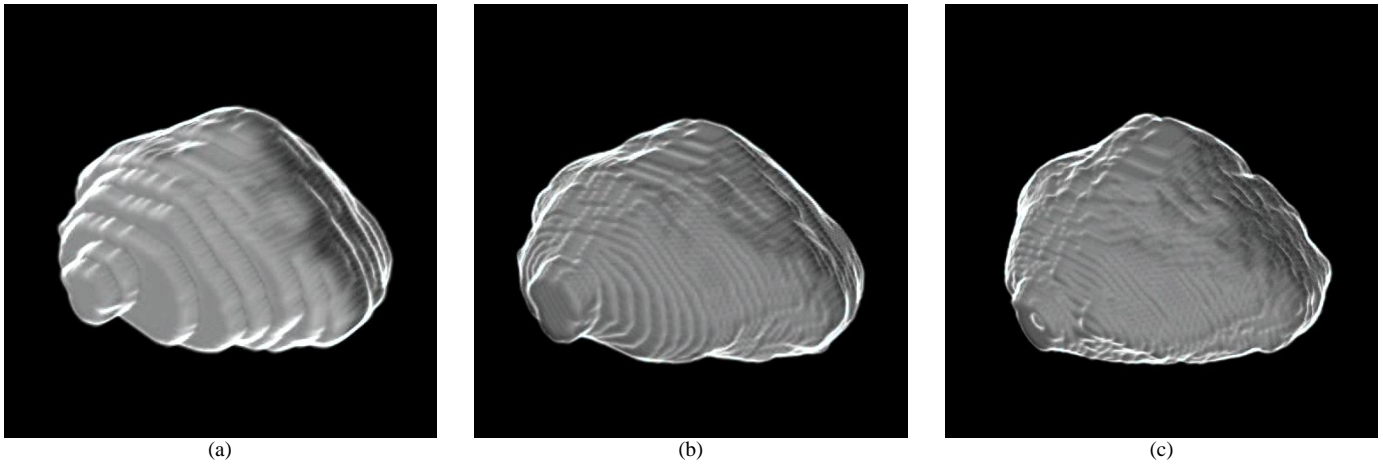


Figure 4. Results of our composite segmentation upsampling procedure. (a) Original axial segmentation of the prostate. (b) Upsampled result for the axial segmentation. (c) Composite result from a combination of the three shape interpolated upsampled segmentation volumes (axial, coronal, and sagittal). The composite segmentation is significantly less faceted and better illustrates the true shape of the prostate.

it will have good resolution in x and y , but poor in z , and thus the segmentation might be off slightly in that dimension. However, the coronal volume will have good resolution in x and z , while the sagittal volume will have good resolution in y and z . In this way, each dimension will be encompassed by the good intra-slice resolution data from two volumes.

For this composite labelmap, we take the axial T_2 -weighted upsampled labelmap as the coordinate system that we will use. For each voxel in the composite volume, an average labelmap is computed using the labelmap values from the three upsampled labelmaps. Only areas where either two or all three segmentations agree are preserved. That is, at least two of the three upsampled labelmaps must agree that a voxel is in the prostate in order for it to be labeled as such, helping to remove outliers. This composite labelmap results in a more accurate and visually pleasing representation of the prostatic volume.

VII. RESULTS

The results of our simple prostate upsampling are shown for one dataset in Fig. 4. The voxel spacing from the original image sequences is $0.55 \times 0.55 \times 3$ mm for each of the sequences (axial, sagittal, and coronal). For this resolution of data, the upsampling interpolation will be performed twice for each of the three T_2 -weighted image volumes, yielding an inter-slice resolution of 0.75 mm. Fig. 4(a) shows an isosurface rendering of the original segmented prostate from the T_2 -weighted axial image sequence. Due to the large inter-slice gap, very obvious plateaus are visible where each slice was segmented. Fig. 4(b) shows a rendering of the result from upsampling the axial sequence alone. The plateau artifacts have been greatly reduced, though are still somewhat disturbing. Fig. 4(c) shows a rendering of the final composite segmentation based on combining the upsampling of the axial, sagittal, and coronal sequences. The faceted artifacts have been further reduced, and the entire shape of the prostate is more full and accurate due to the contributions to the shape from the sagittal and coronal views.

VIII. CONCLUSIONS

We have presented a simple method for performing upsampling of prostate volumes based on ternary labelmaps, where the volume is segmented into PZ, CG, and non-prostate regions. This upsampling is based on using three orthogonal T_2 -weighted image sequences (axial, sagittal, and coronal). The first part of the algorithm upsamples each volume individually by interpolating labelmap slices as needed. Given these three upsampled volumes, the second part of the algorithm combines them to create a composite upsampled volume, which will give the best representation of the prostate. We are integrating this technique into our work on prostate visualization to create accurate and visually pleasing volume rendered images.

ACKNOWLEDGMENTS

This work has been supported by NIH grant R01EB7530 and NSF grants IIS0916235, CCF0702699, and CNS-0959979. The MR datasets used in this work were acquired for the ACRIN 6659 study and are provided courtesy of ACRIN.

REFERENCES

- [1] G. J. Grevera and J. K. Udupa. Shape-based interpolation of multi-dimensional grey-level images. *IEEE Trans. on Medical Imaging*, 15(6):881-892, Dec. 1996.
- [2] G. T. Herman, J. Zheng, and C. A. Bucholtz. Shape-based interpolation. *IEEE Computer Graphics and Applications*, 12(3):69-79, May 1992.
- [3] M. R. Hersh, E. L. Knapp, and J. Choi. Newer imaging modalities to assess tumor in the prostate. *Cancer Control*, 11(6):353-357, Nov. 2004.
- [4] M. J. Horner, L. A. G. Ries, M. Krapcho, N. Neyman, R. Aminou, N. Howlader, S. F. Altekruse, E. J. Feuer, L. Huang, A. Mariotto, B. A. Miller, D. R. Lewis, M. P. Eisner, D. G. Stinchcomb, and B. K. Edwards (eds). SEER cancer statistics review, 1975-2006, National Cancer Institute. Bethesda, MD, based on November 2008 SEER data submission, SEER web site, 2009. http://seer.cancer.gov/csr/1975_2006.
- [5] S. P. Raya and J. K. Udupa. Shape-based interpolation of multi-dimensional objects. *IEEE Trans. on Medical Imaging*, 9(1):32-42, March 1990.
- [6] Y. Zhu, S. Williams, and R. Zwiggelaar. Computer technology in detection and staging of prostate carcinoma: A review. *Medical Image Analysis*, 10(2):178-199, April 2006.